OVERVIEW OF HEAT LOADS IN THE LHC

G. Iadarola*, B. Bradu, P. Dijkstal, L. Mether, G. Rumolo, G. Skripka, L. Tavian
CERN, Geneva, Switzerland

Abstract

A consequence of the formation of electron cloud in beam chambers is the deposition of energy on their walls due to electron impacts. In cryogenic devices this can cause a significant heat load for the cryogenics system, posing constraints on machine design and operation

At the LHC this effect is found to be quite strong and needs to be addressed to avoid performance limitations in view of the planned HL-LHC upgrade. Unexpectedly the eight LHC arcs show very different heat loads. These differences, which appeared after the 2013-14 shut-down period, are still unexplained and have been the subject of thorough investigations and characterizations.

This contribution describes the main observations on the heat loads deposited on the arc beam screens with different beam conditions and in different moments of the LHC operational experience.

INTRODUCTION

The Large Hadron Collider (LHC) is a 27-km synchrotron and particle collider in operation at CERN since 2008 [1]. The machine mostly operates with two proton beams, injected with a beam kinetic energy of 450 GeV and then accelerated to collision energy. The design collision energy is 7 TeV but so far only beam energies up to 6.5 TeV have been reached. The beam structure consists of several trains of 25 ns spaced bunches, allowing a maximum of about 2800 circulating bunches per beam. The nominal bunch population is 1.15×10^{11} p/bunch.

The LHC has an eight-fold symmetric structure, with eight Long Straight Sections (LSS) that host the physics detectors and other equipment, and eight arcs (or sectors). Each arc is 2.5 km long and is made of 23 regular FODO cells, each made of two "half-cells". Each half-cell is 53 m long and is made of one 3.1 m long superconducting quadrupole and three superconducting dipoles, each 14.3 m long, together with much shorter corrector magnets.

Figure 1 shows a cross section of the LHC main dipole. To avoid too large power deposition on the superconducting coils, a beam screen is inserted inside the 1.9 K cold bore, in order to intercept beam-induced heat loads due to RF heating, synchrotron radiation and e-cloud. The beam screen is made of stainless steel with a thin co-laminated copper layer needed to minimize the beam-coupling impedance. It is held by low-conductivity supports and is actively cooled with a helium flow to operate in the range 5-20 K [2]. By measuring the thermodynamic properties of the helium, it is possible to know the heat load deposited on the screen [3]. Magnets in each half-cell share the same cooling circuit, therefore in general only the total heat load on each half-cell can be measured, not the load on individual magnets.

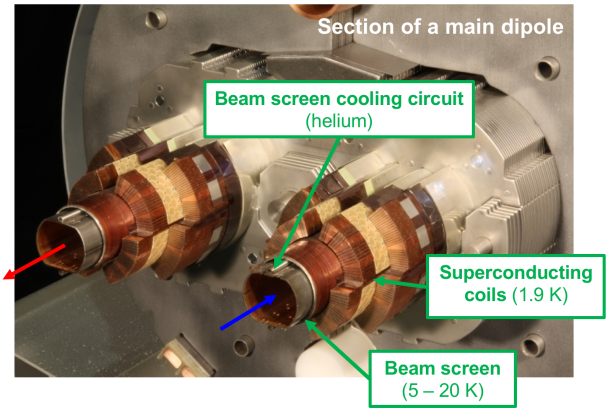

Figure 1: A cut of an LHC dipole magnet.

HEAT LOAD OBSERVATIONS

The history of the LHC operation can be divided in three main periods [4]:

- **Run 1** (2010-2013) was first physics data-taking period. The beam energy was limited to 4 TeV, the bunch spacing was 50 ns, the maximum number of bunches in collision was 1380, the bunch population was gradually increased up to 1.7×10^{11} p/bunch.
- **Long Shutdown 1** (LS1, 2013-2015). In this period no beam operation took place, in order to allow for consolidation and maintenance of the machine equipment. All arcs were warmed up to room temperature and all their beam screens were exposed to air.
- **Run 2** (2015-2018) was second physics data-taking period. The beam energy was increased to 6.5 TeV, the bunch spacing was 25 ns, the maximum number of bunches in collision was 2556, the bunch population was around 1.2×10^{11} p/bunch.

The heat loads observed on the arc beam screens during typical physics runs were very different between Run 1 and Run 2. In Run 1 heat loads were very modest, in the order of 10 W/half-cell, which is compatible with what is expected from impedance and synchrotron radiation heating. Moreover in this period the heat loads in the eight arcs were very similar.

During Run 2, instead, the heat loads became much larger, exceeding 100 W/half-cell. This required the implementation of dedicated feed-forward controls on the cryogenic system regulations [5,6]. The measured heat load were much

* Giovanni.Iadarola@cern.ch

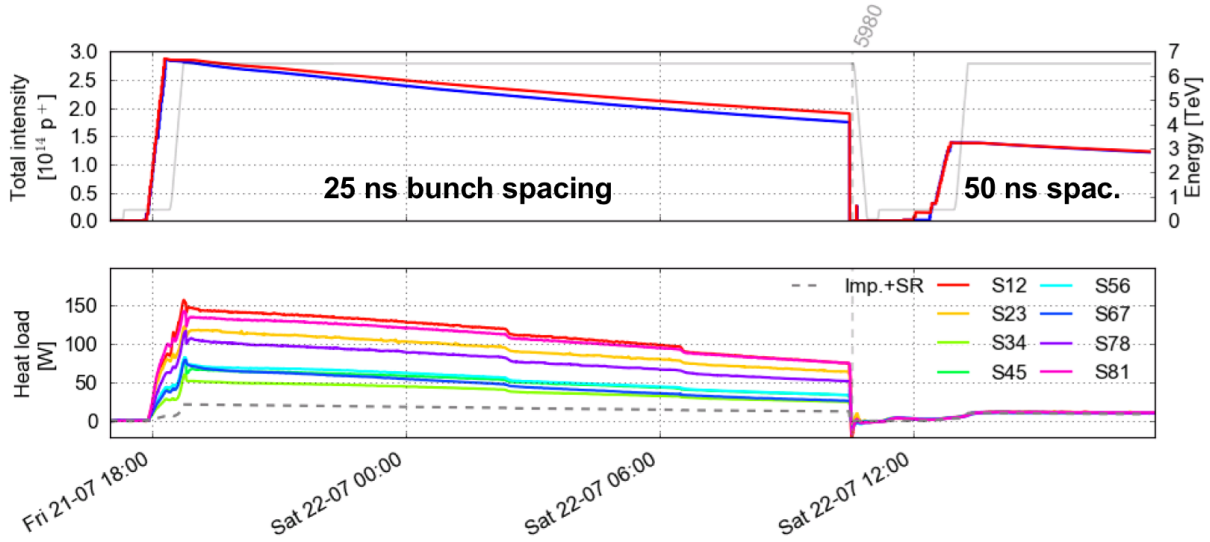

Figure 2: Intensities of the two LHC beams (top) and evolution of the heat load in the eight arcs (bottom) during two consecutive fills with different bunch spacing. Heat load values are in Watts per half-cell. The expected load from impedance and synchrotron radiation is indicated by the dashed curve.

larger than estimated from impedance and synchrotron radiation, suggesting a significant contribution from e-cloud effects. Unexpectedly, very large differences (up to a factor of 3) are observed among the eight arcs (as it is visible in Fig. 2), in spite of the fact that they are by design identical. A detailed description of the heat load observations during Run 2 can be found in [7].

Dedicated tests showed that, as expected from e-cloud simulations [8], such a radical change was caused by the reduction of the bunch spacing from 50 ns to 25 ns. Figure 2 shows two consecutive fills conducted during Run 2. The first is a regular physics production fill performed with 25 ns bunch spacing while the second is a test fill performed with 50 ns bunch spacing. For the 25 ns fill, the heat loads are much larger than expected from impedance and synchrotron radiation heating and large differences are observed among the arcs. For the 50 ns fill instead, the measurements are compatible with the model including only the impedance and the synchrotron radiation contributions and no significant differences among sectors are observed.

The evolution of the heat loads has been closely monitored during the entire Run 2. Figure 3 shows the average heat load measured in the eight arcs at 450 GeV normalized to the circulating beam intensity, for all p-p physics fills of Run 2 performed with more than 800 bunches. A reduction of the heat loads due to beam conditioning is visible mainly in 2015 and in the first part of 2016. After that, practically no further evolution took place. Remarkably, large differences among the arcs remained very visible and were not affected by beam-conditioning accumulated in the period 2016-2018.

The heat loads are distributed very unevenly along the machine. It is possible to identify two families: a group of high-load sectors (including S12, S23, S78, S81) and a group of low-load sectors (including S34, S45, S56, S67). Interestingly, the high-load sectors are contiguous: in fact the machine is practically split in two parts. Especially in the high-load sectors, large differences are observed also among half-cells [9].

It is possible to show that the power deposited in the form of the heat load ultimately comes from the beam. To do so the power lost by the beam can be inferred from RF stable phase measurements and it is found to be consistent with heat load measurements from the cryogenics. RF stable phase measurements also provide the bunch-by-bunch power loss. The characteristic pattern from the e-cloud is clearly visible: the heat load is generated mainly by bunches at the tail of the trains [7, 9].

These observations pose significant concerns in view of the planned upgrade of the LHC (High Luminosity LHC project - HL-LHC), which foresees, together with several hardware upgrades, a twofold increase of the bunch population. The cooling capacity from the cryogenic system available for the arc beam screens in the HL-LHC era is expected to be the same as for the present operation [10]. The present and the HL-LHC operation scenarios are compared in Fig. 4. In the present configuration, the heat loads from impedance and synchrotron radiation are relatively small (in the order of 1 kW per arc), leaving a large fraction of the cooling capacity available to cope with the additional heating from the e-cloud. In the high-load sectors, this available margin is almost fully utilized (as illustrated in Fig. 4 for the Sector 12), while in the low-load sectors less than half of the available capacity is required (as illustrated in Fig. 4 for the Sector 34). The situation is significantly different for the HL-LHC case in which, mainly due to the increase in bunch population, the expected heating from impedance and synchrotron radiation is much larger (almost 4 kW) leaving much less margin to cope with the e-cloud.

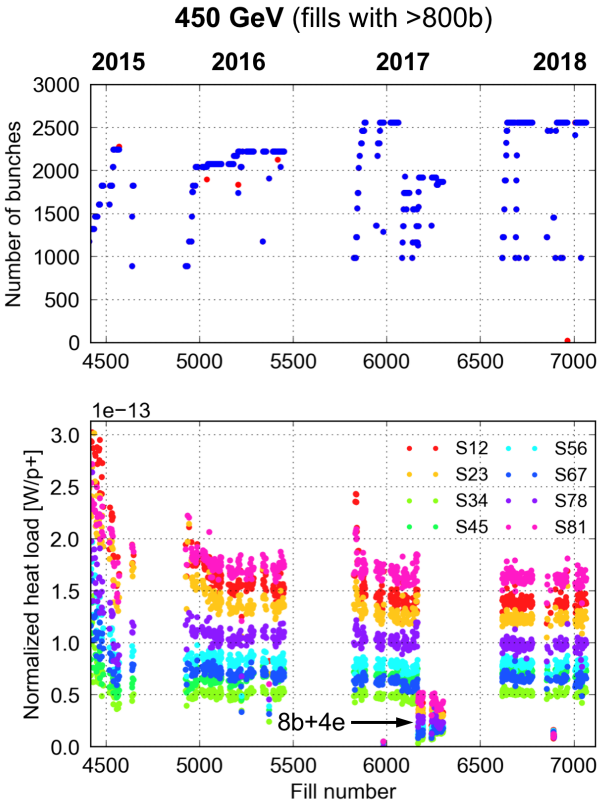

Figure 3: Evolution of the heat loads in the eight LHC arcs during Run 2. Values are in Watts per half-cell and normalized with the circulating beam intensity. The period at the end of 2017 showing lower heat loads was conducted with a special bunch pattern consisting in short trains of eight bunches interleaved with gaps made of four empty slots.

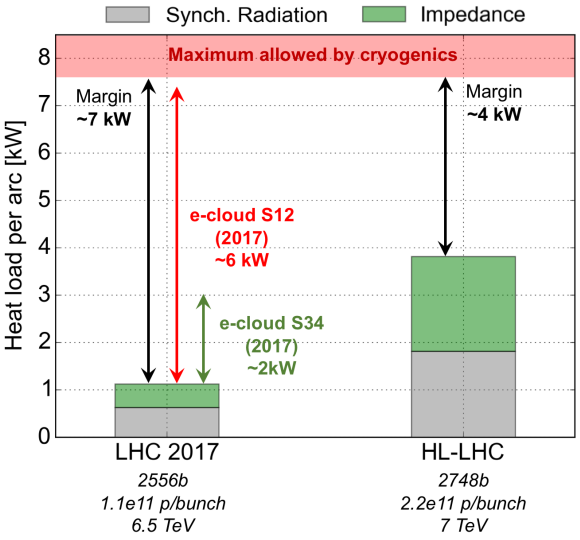

Figure 4: Expected heat loads in the LHC arcs in the present configuration and for the HL-LHC upgrade. The black arrows represent the available margin with respect to the available cooling capacity from the cryogenic system. The red and green arrows represent the heat loads from e-cloud presently observed in a low-load and in a high-load sector respectively.

EFFECT OF VENTING AND THERMAL CYCLES

The observed differences among LHC sectors were not always present.

A test period with 25 ns beams took place at the end of Run 1, in 2012. The heat loads measured during this period can be directly compared against Run 2 data, as the measurement system was largely unchanged and the beam conditions were very similar [11].

A comparison between two very similar fills performed before and after LS1 is shown in Fig. 5. The differences among sectors appeared only after the LS1, during which all arcs were warmed up to room temperature and exposed to air. It is possible to notice that still in 2018, after multiple years of conditioning of the beam chambers, the heat load in the worse sectors is four times larger than before LS1. So far, no difference in the activities conducted during LS1 in the eight sectors could be identified, which could explain this different behaviour in terms of heat load.

During Run 2, in particular during the 2016-17 winter shutdown, the sector 12 had to be warmed-up to room temperature and exposed to air in order to replace a faulty main magnet. The immediate effect of this operation is visible in Fig. 6. As expected a large de-conditioning was observed in Sector 12, which is visible in all half-cells (see Fig. 7 - top). In Fig. 6 one can also notice that the heat loads in the other sectors, which remained under vacuum and at cryogenic temperature, stayed practically unchanged.

Seven days were allocated at the beginning of 2017 for a dedicated scrubbing run at injection energy with the main objective of re-conditioning Sector 12. The evolution of the heat loads during this period is illustrated in Fig. 8, which also shows how the bunch number and the length of the bunch-trains were increased during the scrubbing period. A clear conditioning effect is visible on Sector 12 over the first four days, after which the heat loads had reached levels similar to end-2016, i.e. before the warm-up (as it can be seen at a cell-by-cell level in Fig. 7 - bottom). No further evolution was observed thereafter, and in particular it was not possible to reduce the heat loads to levels similar to 2012.

Comparing these observations with those made before and after LS1, we notice that the effect of LS1 was somehow more permanent than the effect of the 2016-17 venting. The reasons of this behaviour are presently under investigation [12, 13].

COMPARISON OF THE MEASUREMENTS AGAINST MODELS AND SIMULATIONS

Electron cloud is the only identified heating mechanism that is found to be compatible with the observations [9]. The most characteristic features are the following:

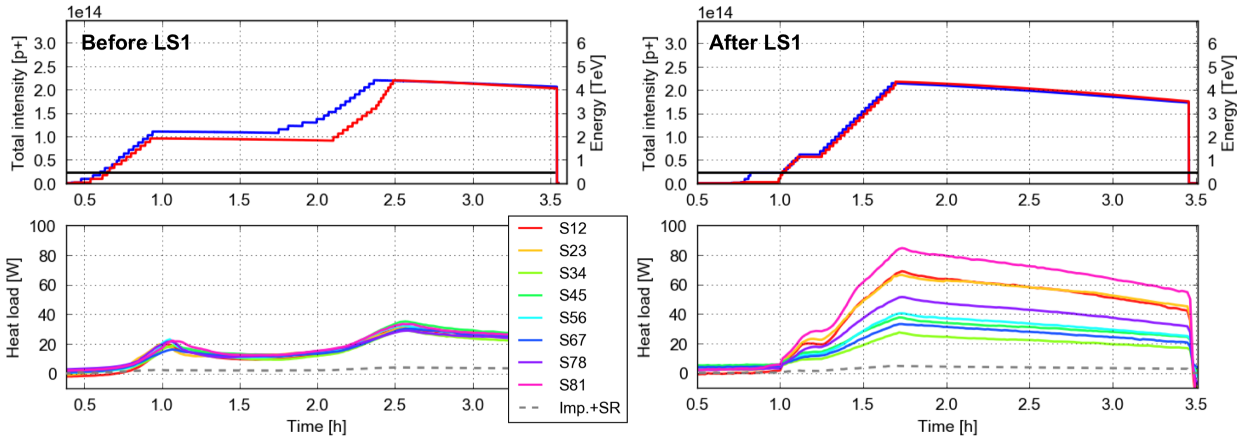

Figure 5: Beam intensities (top) and heat loads measured in the eight LHC arcs (bottom) measured during two fills conducted with the same filling pattern in 2012 (left) and in 2018 (right). Heat load values are in Watts per half-cell.

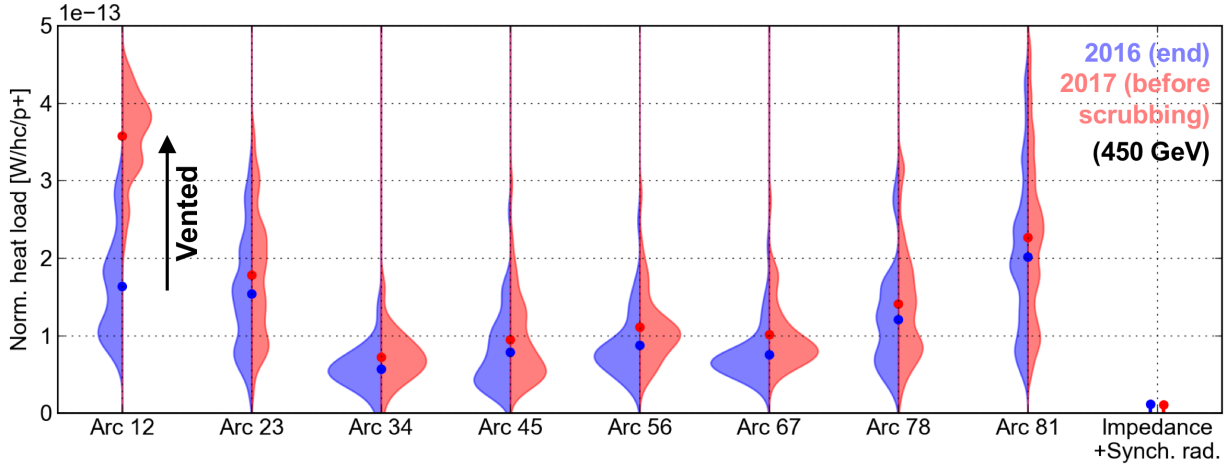

Figure 6: Average (dots) and cell-by-cell distribution in the eight arcs before and after the 2016-17 winter shut-down. The effect of the air exposure for the beam screens in sector 12 is clearly visible. Heat load values are in Watts per half-cell and normalized by the circulating beam intensity.

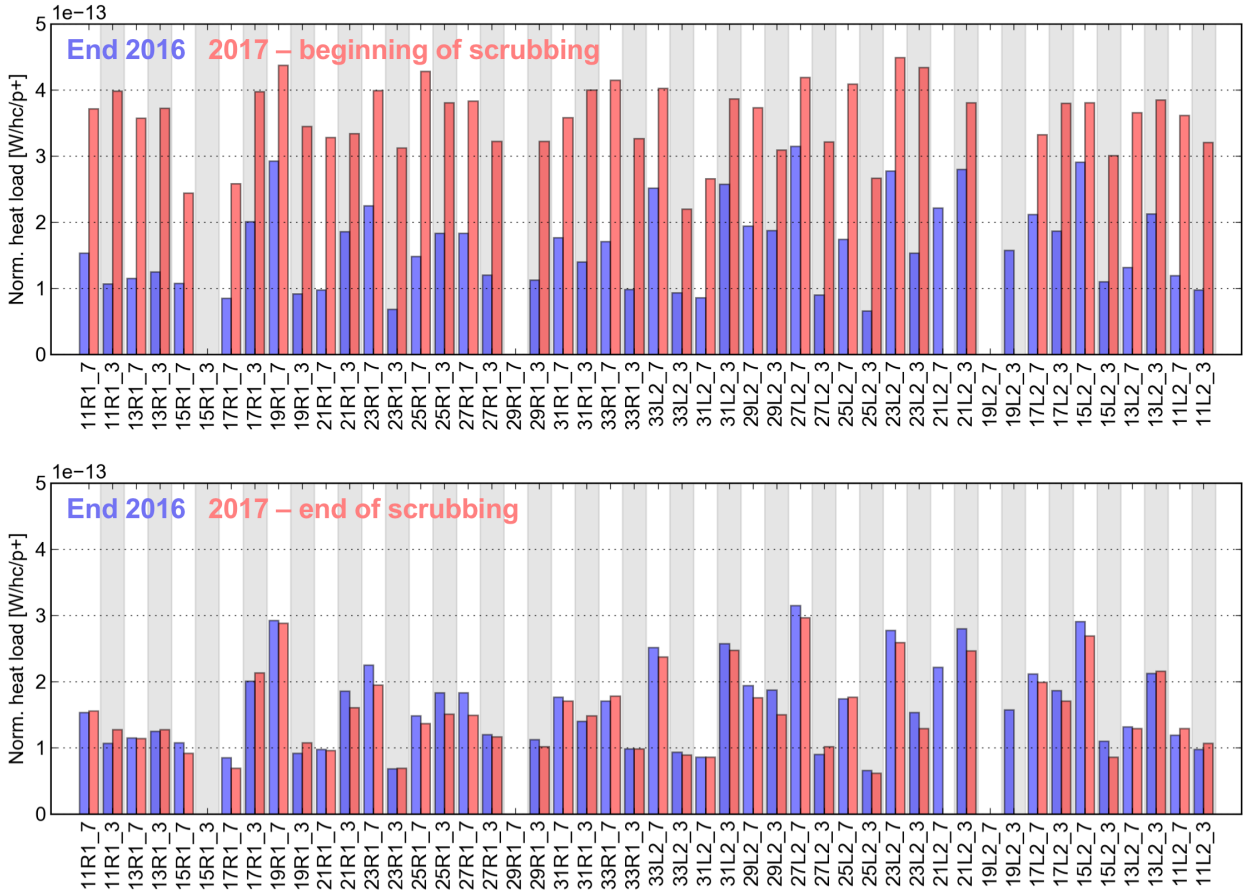

Figure 7: Heat loads in all half-cells of sector 12 as measured at the end of 2016 (in blue) and at the beginning and end of the 2017 scrubbing run (in red in the top and bottom plots respectively). Heat load values are in Watts per half-cell and normalized by the circulating beam intensity.

- Heat loads significantly larger than impedance and synchrotron radiation estimates are visible only with the 25 ns bunch spacing;
- Measurements taken with 25 ns beams and different bunch intensity show the existence of an intensity threshold around 0.4×10^{11} p/bunch;
- Large heat loads and heat load differences among sectors are already present at injection energy (450 GeV) and increase only moderately during the energy ramp. It is unlikely that photoelectrons from synchrotron radiation play a major role in generating the observed differences, as they should show a very strong dependence on the beam energy.

In Fig. 9 we compare the measured heat loads (on the right) against the result of e-cloud buildup simulations performed with the PyECLOUD code [14], for different $\mathrm{SEY}_{\mathrm{max}}$ parameters. The model used for these simulations is described in detail in [15, 16].

Assuming that the differences in heat load are caused by differences in SEY, we observe that the average heat load measured in the low-load sectors is compatible with $\mathrm{SEY}_{\mathrm{max}}$=1.25 while the average heat load measured in the high-load sectors is compatible with $\mathrm{SEY}_{\mathrm{max}}$=1.35. We also observe that for the half-cells showing the highest load the estimated $\mathrm{SEY}_{\mathrm{max}}$ can be as high as 1.50.

INFORMATION FROM SPECIAL INSTRUMENTED CELLS

As already mentioned, in most of the LHC arc half-cells temperature sensors on the beam screen cooling circuit are available only at the entrance and at the exit of the half-cell, therefore only the total load deposited over the entire half-cell length is known.

A small selection of arc half-cells have been equipped with additional thermometers to allow measuring the heat load on each magnet:

- Three half-cells in sector 45 were instrumented during LS1 and they always showed relatively low heat loads during Run 2.
- One half-cell in sector 12, the half-cell 31L2 which was showing higher heat loads in 2015-16, was instrumented during the 2016-17 winter shut-down, when one of its magnets had to be exchanged.

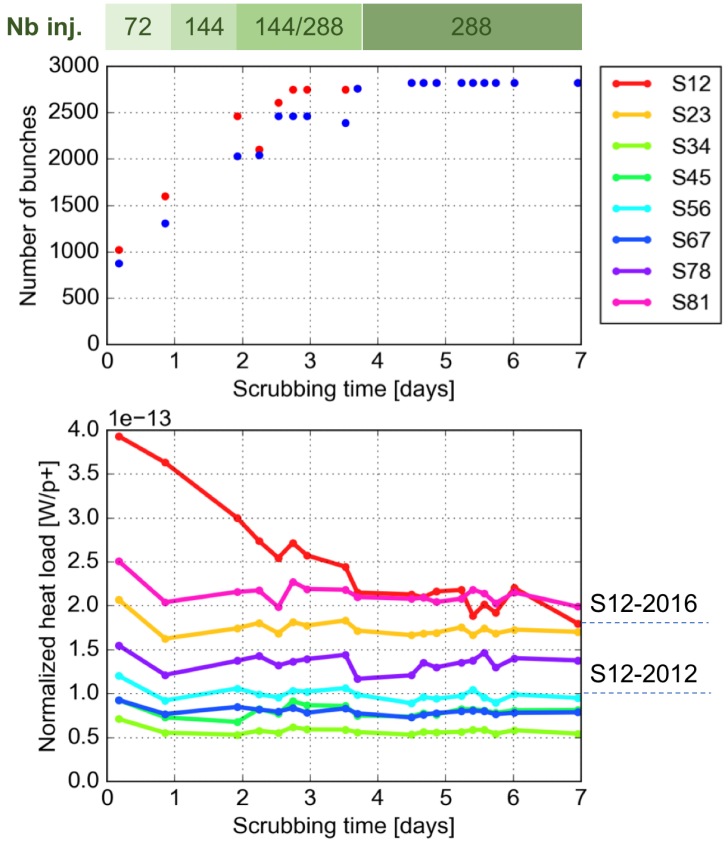

Figure 8: Evolution of beam configuration (top) and heat loads in the LHC arcs (bottom) during the 2017 scrubbing run. Heat load values are in Watts per half-cell and normalized by the circulating beam intensity. The values that had been measured for sector 12 in 2012 and in 2018 are marked on the side of the plot.

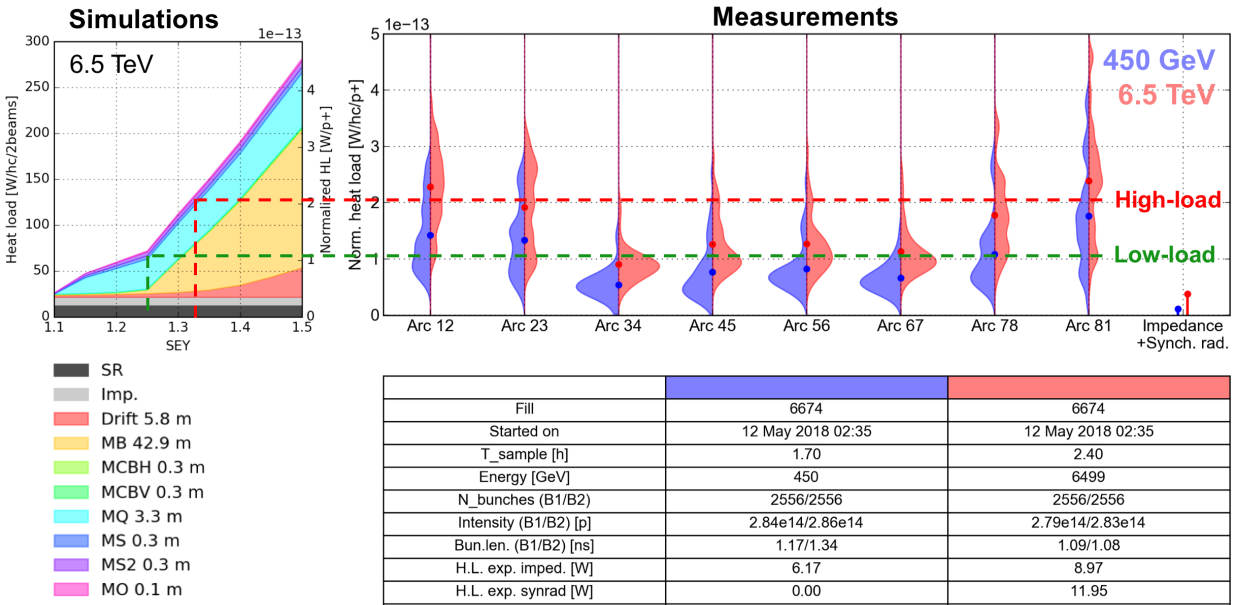

Fill	6674	6674
Started on	12 May 2018 02:35	12 May 2018 02:35
T_sample [h]	1.70	2.40
Energy [GeV]	450	6499
N_bunches (B1/B2)	2556/2556	2556/2556
Intensity (B1/B2) [p]	2.84e14/2.86e14	2.79e14/2.83e14
Bun.len. (B1/B2) [ns]	1.17/1.34	1.09/1.08
H.L. exp. imped. [W]	6.17	8.97
H.L. exp. synrad [W]	0.00	11.95
H.L. exp. imp.+SR [W/p+]	1.08e-14	3.72e-14
T_nobeam [h]	1.15	1.15

Figure 9: Heat loads from PyECLOUD simulations (left) compared against measurements from a typical fill of the 2018 run (right).

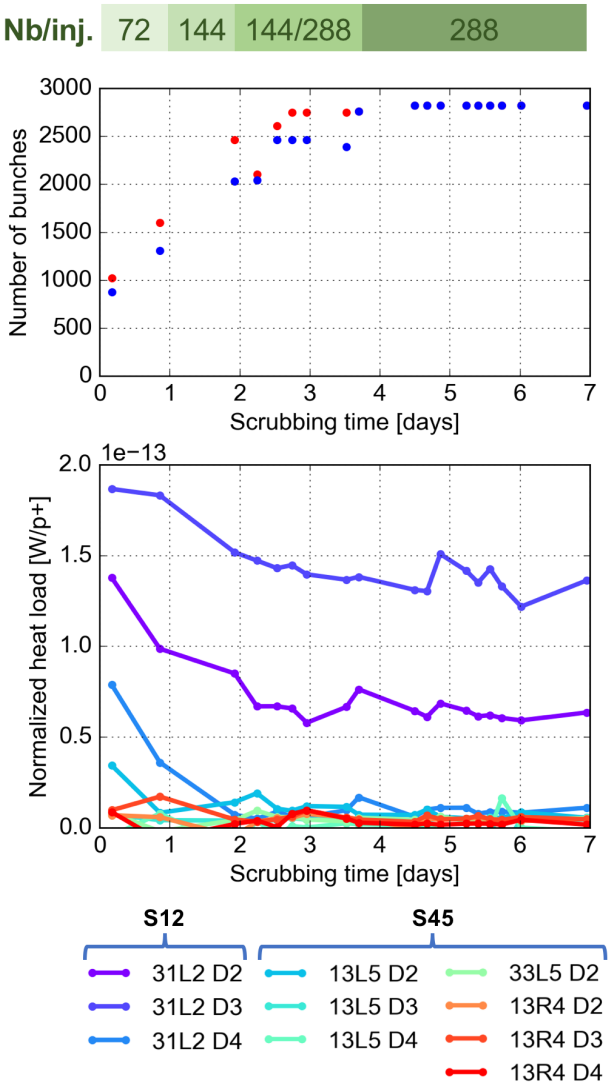

Figure 10: Evolution of beam configuration (top) and heat loads in the instrumented dipoles (bottom) during the 2017 scrubbing run. Heat load values are in Watts per half-cell and normalized by the circulating beam intensity.

It is particularly interesting to look at the evolution of the heat loads in the magnets of the cell 31L2 right after the thermal cycle and air exposure which took place in the 2016-17 winter shut-down, when the dipole "31L2-D4" was exchanged.

As shown in Fig. 10, very low heat loads were measured on the dipoles in sector 45 which had not been exposed to air during the winter shut-down. The newly installed dipole "31L2-D4" conditioned very rapidly to the same level as those in S45. The other two dipoles in the same half-cell ("31L2-D2" and "31L2-D3"), which are installed since the time of the LHC construction, surprisingly show much larger heat loads even after a long period of conditioning. Most likely magnets with a similar behaviour are present also in the other high-load half-cells.

SUMMARY AND FUTURE PLANS

During Run 2, large heat loads are observed on the arc beam screens of the LHC when operating with 25 ns bunch space spacing, which are worrisome for the HL-LHC upgrade.

These heat loads are very different from arc to arc, from cell to cell and from magnet to magnet. The origin of these differences is still unknown and is the subject of several investigations.

Such large differences appeared only after the 2013-14 shut-down, in which the beam screens of all the arcs were warmed-up and exposed to air, but no further change was observed when the air exposure was repeated on one of the sectors in the 2016-17 winter shutdown.

Electron cloud effects are the only identified mechanism that is compatible with experimental observations like the dependence on the bunch spacing, the dependence on the bunch intensity, the bunch-by-bunch pattern on beam power loss (measured by the RF system).

Efforts are ongoing to further localize the heat load within the magnet length, using the temperature evolution observed in the instrumented half-cells at the re-cooldown after a beam dump. For this purpose during the upcoming Long Shutdown 2 (LS2) mass flow-meters will be installed to reduce the uncertainty on the measurement of the helium flow. During LS2 magnets extracted from the LHC will undergo extensive analysis aiming at identifying the origin of the observed heat load differences. Moreover, additional half-cells will be instrumented in preparation for the 2021-23 run.

ACKNOWLEDGMENTS

The authors would like to thank all members of the CERN Beam-Induced Heat Loads Task Force, G. Arduini, F. Giordano, E. Metral, and B. Salvant for their important input to the present contribution.

REFERENCES

[1] O. Bruning, P. Collier, P. Lebrun, S. Myers, R. Ostojic, J. Poole, and P. Proudlock (editors), "LHC Design Report, Volume 1." CERN-2004-003-V-1, 2004.

[2] E. Hatchadourian, P. Lebrun, and L. Tavian, "Supercritical Helium Cooling of the LHC Beam Screens," *LHC Project Report*, vol. 212, 1998.

[3] K. Brodzinski and L. Tavian, "First Measurements of Beam-Induced Heating on the LHC Cryogenic System," Tech. Rep. CERN-ATS-2013-009, CERN, Geneva, Jan 2013.

[4] J. Wenninger, "LHC status and performance," *PoS*, vol. CHARGED2018, p. 001, 2019.

[5] B. Bradu, A. Tovar González, E. Blanco Viñuela, P. Plutecki, E. Rogez, G. Iadarola, G. Ferlin, and B. Fernández Adiego, "Compensation of beam induced effects in LHC cryogenic systems," in *Proc. of International Particle Accelerator Conference (IPAC'16), Busan, Korea, May 8-13, 2016*, 2016.

[6] B. Bradu, "How does a cryogenic system cope with e-cloud induced heat load? what can we learn from heat load measurements?." These proceedings.

[7] G. Iadarola, G. Rumolo, P. Dijkstal, and L. Mether, "Analysis of the beam induced heat loads on the LHC arc beam screens during Run 2," *CERN-ACC-NOTE-2017-0066*, Dec 2017.

[8] O. Domínguez, K. Li, G. Arduini, E. Métral, G. Rumolo, F. Zimmermann, and H. M. Cuna, "First electron-cloud studies at the large hadron collider," *Phys. Rev. ST Accel. Beams*, vol. 16, p. 011003, Jan 2013.

[9] G. Iadarola, "Electron cloud and heat loads in the LHC arcs." Accelerator and beam physics forum, CERN, 12 Jul 2018 https://indico.cern.ch/event/740046.

[10] G. Apollinari, I. Bejar Alonso, O. Bruning, P. Fessia, M. Lamont, L. Rossi, and L. Tavian, *High-Luminosity Large Hadron Collider (HL-LHC): Technical Design Report V. 0.1*. CERN Yellow Reports: Monographs, Geneva: CERN, 2017.

[11] G. Iadarola, "Head loads in run 1 and run 2." Presentation at the LHC Machine Committee, CERN, 12 Sep 2018 , available at https://indico.cern.ch/event/756722/.

[12] L. Tavian, "Report from the task force on beam induced heat load." Presentation at the LHC Performance Workshop 2018, Chamonix, Jan 2018.

[13] V. Petit, "Characterisation of beam screens extracted from lhc magnets." These proceedings.

[14] G. Iadarola, E. Belli, K. Li, L. Mether, A. Romano, and G. Rumolo, "Evolution of Python Tools for the Simulation of Electron Cloud Effects," in *Proc. of International Particle Accelerator Conference (IPAC'17), Copenhagen, Denmark, May, 2017*, JACoW.

[15] P. Dijkstal, G. Iadarola, L. Mether, and G. Rumolo, "Simulation studies on the electron cloud build-up in the elements of the LHC Arcs at 6.5 TeV," *CERN-ACC-NOTE-2017-0057*, Oct 2017.

[16] P. Dijkstal, "Investigating the role of photoemission in the e-cloud formation at the lhc." These proceedings.